DYNAMIC NEGATION OF BASIC BELIEF ASSIGNMENTS IN DEMPSTER-SHAFER THEORY WITH APPLICATIONS IN CLASSIFICATION AND LOW-LIGHT IMAGE ENHANCEMENT

Anonymous authors
Paper under double-blind review

ABSTRACT

The effective modelling of uncertain information is the key to improving the level of decision-making. Dempster-Shafer theory (DST) can express unknown and partial reliability explicitly. However, existing methods based on DST focus mostly on the accumulation of positive evidence and ignore the counterbalancing effect of negative evidence on the belief distribution, which leads to one-sidedness of decision-making in scenarios of intensified conflict. To this end, this paper proposes a dynamic negation of basic belief assignment (DNBBA), which measures the strength of refutation. In addition, we analyse the properties of DNBBA. On this basis, a decision-making network based on DNBBA (DNBBA-DNet) is proposed, which achieves the migration of the decision paradigm from positive accumulation to dialectical checks and balances. The experimental results demonstrate that the proposed method outperforms state-of-the-art methods on benchmark datasets, enhancing the classification accuracy and overall performance of low-light image enhancement (LLIE) tasks.

1 INTRODUCTION

Because of the inevitable existence of uncertain information, uncertainty is a fundamental challenge in the process of constructing complex models for decision-making. The systematic representation and reasoning of uncertainty not only help deepen the understanding of potential disturbance mechanisms but also significantly enhance the robustness and accuracy of decision-making. Therefore, effective processing of uncertainty information has become the key to decision-making. Many methods have been proposed to solve this problem, such as fuzzy sets (Rani et al., 2024), Bayesian inference (Liu et al., 2025), evidence theory (Fan et al., 2025a), complex evidence theory (Xiao, 2020), and deep learning models (Li et al., 2022a), which have been applied in several fields, such as object detection (Li et al., 2026), graph clustering (Zhang et al., 2022b), and pattern classification (Huang et al., 2025b; Sun et al., 2026). However, how to handle uncertain information effectively remains a key and challenging issue.

Many machine learning models have been proposed to classify tabular data for decision-making, including k-nearest neighbor (KNN) (Cover & Hart, 1967), decision tree (REPTree) (Freund & Mason, 1999), nearest mean classifier (NMC) (Veenman & Reinders, 2005), support vector machine (SVM) (Chang & Lin, 2011), and cost-sensitive algorithm (CSMLP) (Castro & Braga, 2013). Despite the emergence of various methods in recent years that improve classification accuracy, the problem of information uncertainty has yet to be effectively addressed. Dempster-Shafer theory (DST) quantifies uncertainty by introducing a basic belief assignment. Unlike traditional probability theory, DST allows partial uncertainty to exist and is more flexible in dealing with uncertainty from multisource information. Recently, He et al. (2021) proposed a learning-based basic belief assignment (BBA) modelling framework tailored for attribute-based interval evidence. This approach employs training samples to drive data-adaptive optimisation of hyperparameters within traditional interval BBA models, thereby yielding more discriminative belief allocations in classification fusion tasks. Li et al. (2024b) further proposed a learning-based multimethod fusion of the BBA (LBMMF) mechanism. This approach directly learns the mapping from raw samples to the composite BBA

Reviewers: please read the Reviewer Guidelines (iclr.cc/Conferences/2027/ReviewerGuidelines) and the AI Policy for Reviewers (iclr.cc/Conferences/2027/AIPolicyForReviewers). If you used AI to expand, edit, or polish your review, please provide the input text to the LLM. Better still, consider skipping the LLM and submitting your original text: we, and the authors, are much more interested in your unedited thoughts than in what an LLM has to say. AI-assisted or not, you are putting your name and reputation behind your review: LLM-generated falsehoods, hallucinations or misrepresentations are subject to disciplinary action, which may include desk-rejecting all papers you have authored.

through end-to-end training of deep networks; the composite BBA is jointly generated by several mainstream BBA construction strategies, effectively enhancing evidence reliability and classification accuracy. Xiao (2020) theoretically extended Dempster-Shafer evidence theory by generalising the domain of the quality function to complex numbers and proposing complex-valued basic belief assignment (CBBA). This generalised evidence theory demonstrated superior expressiveness for uncertain information in pattern classification scenarios, thereby improving classification performance. In addition, numerous approaches (Li et al., 2022a; Park et al., 2024; Li et al., 2024a) have used DST to improve the accuracy of classification in recent years, but these methods still have the following disadvantages:

- Existing methods based on DST focus mainly on the accumulation of positive evidence and fail to effectively introduce the reverse regulatory mechanism of negative evidence on the belief distribution during the belief allocation process, which is prone to bias in the results of decision-making.
- Existing studies on DST focus mainly on conflict measurement and fusion rule improvement between evidence and rarely construct a directional and asymmetric similarity measurement mechanism starting from the structural differences between propositions, which limits the accuracy and interpretability of belief revision.
- After the basic belief assignment (BBA) is determined, the traditional DST method usually adopts a static fusion strategy to make a decision, which lacks modelling of the dynamic evolution mechanism of the belief structure and has difficulty adapting to uncertain changes in evidence in complex environments.

To address these problems, we propose a dynamic negation of basic belief assignment (DNBBA), which involves the construction of an asymmetric similarity kernel to adaptively measure the refutation strength in the proposition difference space to realize the negative revision of the original belief. We also analyse and discuss the properties of the DNBBA and present the results of the negation iteration through an example. Finally, the proposed DNBBA is incorporated into an end-to-end decision framework, enabling the unified and joint optimization of classification and enhancement tasks under the minimum negative belief criterion. In summary, the main contributions of our work are as follows:

- We propose DNBBA, which introduces a learnable asymmetric similarity function, overcoming the limitations of traditional DST, which relies only on positive evidence. The bidirectional dynamic correction of the belief distribution is realized, which effectively alleviates the decision bias caused by class imbalance and evidence conflict.
- We systematically analyse the mathematical properties of the DNBBA theoretically, derive its convergence formula for multiple negation iterations, and prove that it tends toward a uniform distribution at the limit.
- Based on DNBBA, we further propose a decision-making network (DNBBA-DNet) to drive the coevolution of support and refutation on the evidence manifold. We verify that our method improves the overall performance of image classification and low-light image enhancement tasks on multiple benchmark datasets.

2 Related Work

2.1 Evidence Theory-based Methods of DST

As the need for robustness in classification and reliability in uncertainty estimation continues to intensify, evidential learning has evolved into a more mature and systematic research paradigm. Xu et al. (2013) proposed a novel method (NDC) to determine basic probability assignment (BPA) in DST by building models based on a normal distribution for each attribute of the data, effectively handling non-normal data and missing values to improve classification accuracy. Xiao et al. (2023) introduced a generalised divergence-based decision-making method (DMA) that utilises new evidential divergence measures and a weighted belief Jensen-Shannon divergence to improve conflict management and decision accuracy in pattern classification. Xiao et al. (2025) proposed a decision method based on generalised f-divergence, which utilises a new measure of evidence divergence

and can be decomposed into different evidence measurement methods according to different kernel functions. These new evidence divergence measures are able to quantify the difference between belief functions in Dempster-Shafer evidence theory. Huang et al. (2024) proposed a new fractal belief Rényi (FBR) divergence and developed a multisource information fusion algorithm for pattern classification. FBR divergence is the first extension of the fractal concept to Rényi divergence, which can effectively measure the difference in evidence evolution over time. However, these methods have not been studied from a negative perspective and rely only on the basic reliability assignment of positive support, which can lead to one-sidedness in decision-making.

2.2 Deep Learning-based Methods of DST

In recent years, the integration of Dempster-Shafer theory (DST) with deep learning models has shown potential for enhancing classification performance by effectively managing uncertainty and ambiguity. Zheng et al. (2021) proposed an evidential classifier (DSC) that integrates DST with convolutional neural networks to achieve set-valued classification, demonstrating improved performance in handling uncertainty and ambiguity. Building upon this foundation, Li et al. (2022a) developed a trustworthy long-tailed classification framework (TLC) that embeds uncertainty estimation into a multiexpert architecture, thereby enhancing robustness against class imbalance and mitigating the unreliability of predictions in long-tailed scenarios. Alzahem et al. (2024) further explored the integration of DST with multiple pretrained architectures of convolutional neural networks for feature fusion and demonstrated enhanced classification accuracy on datasets by effectively managing uncertainties through ensemble learning. More recently, Ye et al. (2024) proposed an uncertainty regularised evidential regression method to address limitations in the learning capability of evidential models, particularly in high-uncertainty areas. However, despite these advances, limitations remain in the learning capability of evidential models, particularly in high-uncertainty areas.

3 Preliminaries

The DST is a theoretical framework for addressing uncertain information and is used to express and combine incomplete knowledge. It is based on a discriminative framework of all possible propositions and expresses the degree of support for different propositions through basic belief assignments.
Definition 1 (Frame of discernment). Let Θ be a set of mutually exclusive and nonempty events. The frame of discernment (FOD) is defined as follows:

$$\Theta = \{L_1, L_2, \cdots, L_\xi\}. \tag{1}$$

Definition 2 (Proposition). The power set of Θ is denoted as follows:

$$2^\Theta = \{\emptyset, \{L_1\}, \{L_2\}, \cdots, \{L_\xi\}, \{L_1 \cup L_2\}, \cdots, \Theta\}, \tag{2}$$

where $\emptyset$ is denoted as an empty set. $\tau_i \in 2^\Theta$ is defined as a proposition.
Definition 3 (Basic belief assignment). Let m be a BBA on $\Theta = \{L_1, L_2, \cdots, L_\xi\}$. The BBA is defined as follows:

$$m : 2^\Theta \to [0, 1], \tag{3}$$

and satisfies

$$\begin{aligned} \sum_{\tau_i \in 2^\Theta} m(\tau_i) = 1, \\ m(\emptyset) = 0. \end{aligned} \tag{4}$$

4 Methodology

4.1 Motivation and Overview

In the existing research on uncertain information modelling, although unknown and partial reliability can be expressed explicitly via DST, the existing methods focus mostly on the accumulation of positive evidence and ignore the reverse adjustment effect of negative evidence in the belief distribution,

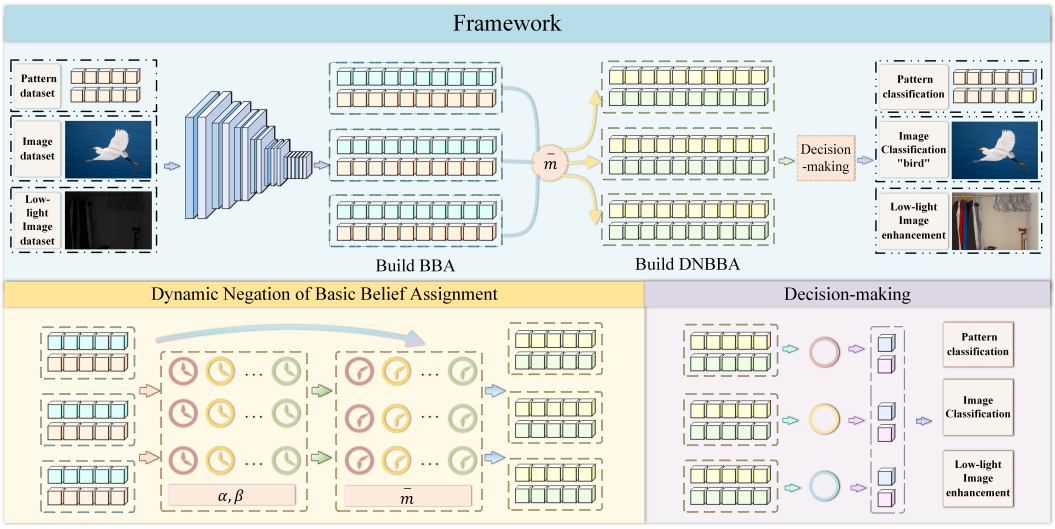

Figure 1: The overall architecture of the proposed DNBBA-DNet. It consists of four main modules: the BBA building module, the DNBBA building module, and the decision-making module.

which leads to deviations in decision scenarios with class-imbalanced distributions or aggravated evidential conflicts. Consequently, we propose DNBBA, which introduces a learnable asymmetric similarity function to measure the strength of support and refutation simultaneously to realize the bidirectional dynamic revision of beliefs. Furthermore, we systematically analyse the mathematical properties of the DNBBA, derive the convergence formula for multiple negation iterations, and prove that its limitation tends toward a uniform distribution. Finally, DNBBA-DNet, which is based on DNBBA, is further constructed to promote the coevolution of support and refutation on the evidence manifold, thereby improving the comprehensive performance of image classification and low-light image enhancement tasks on multiple benchmark datasets.

First, we input datasets X, which generate different basic belief assignments (BBAs) via feature extraction:

$$m^x = \{m_1^x, \cdots m_g^x, \cdots, m_e^x\}, \tag{5}$$

where m_g^x is the value of sample x at the gth BBA. e denotes the number of BBAs.

After that, the negated BBA is obtained by our definition of the DNBBA:

$$\bar{m}_1^x, \cdots \bar{m}_g^x, \cdots, \bar{m}_e^x = \mathrm{DNBBA}(m_1^x, \cdots m_g^x, \cdots, m_e^x), \tag{6}$$

where $\bar{m}_g^x$ is the value of sample x at the gth DNBBA.

Finally, the obtained dynamic negation of basic belief assignments (DNBBAs) are subjected to decision-making (DM) operations to yield the final decision result:

$$\bar{M} = \mathrm{DM}(\bar{m}_1^x, \cdots \bar{m}_g^x, \cdots, \bar{m}_e^x). \tag{7}$$

4.2 Dynamic Negation of Basic Belief Assignment

This subsection presents the DNBBA as well as its theorems, properties, and corollaries. Θ is a set of mutually exclusive and nonempty events. L_ξ is a nonempty event.

Let m be a BBA on $\Theta = \{L_1, L_2, \cdots, L_\xi\}$. The dynamic negation of basic belief assignment is defined as follows:

$$\bar{m}\left(\tau_i\right) = \sum_{\tau_k \subset \Theta} m(\tau_k) \cdot \psi(\tau_i, \tau_k), \tag{8}$$

with

$$\psi(\tau_i, \tau_k) = \frac{\bar{\psi}\left(\tau_i, \tau_k\right)}{\sum_{\tau_i \subset \Theta} \bar{\psi}\left(\tau_i, \tau_k\right)}, \tag{9}$$

$$\bar{\psi}\left(\tau_i, \tau_k\right) = \alpha \cdot \frac{|\tau_i \backslash \tau_k|}{|\tau_i|} + \beta \cdot \frac{|\tau_k \backslash \tau_i|}{|\tau_k|}, \tag{10}$$

and satisfies

$$\begin{aligned} \alpha &= \exp\left(-\rho \cdot |m(\tau_i) - m(\tau_k)|\right), \\ \alpha + \beta &= 1, \\ \bar{m}\left(\emptyset\right) &= 1, \end{aligned} \tag{11}$$

where ρ is the smooth attenuation coefficient and where $|\cdot|$ is the cardinality.

Property 1. The function is nonnegative. $\forall \tau_i, \tau_k, \psi(\tau_i, \tau_k) \geq 0$ and $m(\tau_k) \geq 0$, from which we can derive $\bar{m}\left(\tau_i\right) \geq 0$.

Theorem 1. When $|\tau_i| = 1, \tau_i \cap \tau_k = \emptyset$, the mathematical expression for $\bar{m}\left(\tau_i\right)$ is $\frac{1-m(\tau_i)}{|\Theta|-1}$, and $|\Theta|$ is the cardinality of Θ.

Property 2. The DNBBA has the property of normalisation.

Theorem 2. Let $\bar{m}$ be a double negation of m. The process of the DNBBA is not involutionary when $|\Theta| > 2$, such that $\bar{\bar{m}}\left(\tau_i\right) \neq m(\tau_i)$.

Property 3. DNBBA satisfies linear stability. When $m = \lambda m_1 + (1-\lambda) m_2$ and $\sum_{\tau_k \subset \Theta} \psi(\tau_i, \tau_k) = 1$, $\bar{m} = \lambda\, \bar{m}_1 + (1-\lambda)\, \bar{m}_2$.

Theorem 3. When $|\tau_i| = 1, \tau_i \cap \tau_k = \emptyset$. After the $(\upsilon+1)^{th}$ negation, $\bar{m}_{\upsilon+1} = \frac{1-\bar{m}_\upsilon}{|\Theta|-1} \Rightarrow \bar{m}_\upsilon = (\bar{m}_1 - \frac{1}{|\Theta|})(\frac{1}{1-|\Theta|})^{\upsilon-1} + \frac{1}{|\Theta|}$.

Corollary 1. When $\upsilon \to \infty$, $\bar{m}_i$ becomes a uniform distribution.

Property 4. The value of $\bar{m}\left(\tau_i\right)$ has an upper bound.

Property 5. Since $\psi(\tau_i, \tau_k)$ is asymmetric, $\bar{m}$ is biased toward the direction with the most assignments away from the original. When BBAs are reversed, the information center of gravity shifts to play the role of refutation, which is consistent with the counter-questioning in the DST.

Property 6. The DNBBA inherently tends to increase in entropy. $\psi(\cdot)$ can distribute $m(\tau_k)$ smoothly across multiple τ_i, which makes $\bar{m}$ more dispersed than m and leads to an increase in the entropy of $\bar{m}$.

Property 7. The DNBBA satisfies the principle of minimal self-consistency. When τ_i has all the beliefs, $m(\tau_i) = 1$, $\bar{m}\left(\tau_i\right) = \psi(\tau_i, \tau_i) = 0$, which indicates that the dissimilarity between $m(\tau_i)$ and $m(\tau_i)$ is 0.

Property 8. The DNBBA has boundary behavior.

Property 9. The negation of BBA is sensitive to set differences, and even if the union of two sets is large, the negation of BBA will be small if they have many different elements.

Property 10. The negative value of the BBA for each proposition is independent of the order of the elements in that proposition. More proof details for theorems and properties are provided in the Appendix.

4.3 DECISION-MAKING

Let $\bar{m} = \{\bar{m}_1^x, ..., \bar{m}_g^x, \ldots, \bar{m}_e^x\}$ be different DNBBAs, which are fused via Dempster's rule of combination:

$$\bar{M}^x = \{\bar{m}_1^x \oplus \bar{m}_g^x \oplus \ldots \oplus \bar{m}_e^x\}. \tag{12}$$

The probabilities of different patterns obtained after fusion are prepared for subsequent classification and LLIE tasks. In the classification, the result of the decision for this sample is obtained by selecting the category corresponding to the minimum value:

$$\arg \min_{1 \leq \delta \leq \xi} \{\bar{M}^x\left(L_\delta\right)\}, \tag{13}$$

where L_δ denotes the δth class. In the LLIE task, images are input into the proposed decision-making strategy D_s to obtain a representation of the degradation level for different features of each

Algorithm 1 A decision-making strategy based on DNBBA

Input: Datasets $X = \{X_1, \cdots X_x, \cdots, X_n\}$;
Output: Category probabilistic decision-making results

```
for g = 1; g ≤ e do
    for x = 1; x ≤ n do
        Obtain BBAs based on the data attribute features of X;
        Obtain the DNBBA based on the BBA;
    end for
end for
for g = 1; g ≤ e do
    Obtain the fused DNBBA by Eq. (12);
end for
Use the decision results for subsequent tasks
```

pixel in the image I_p. A smaller value indicates a lower degradation level and is assigned a smaller weight, which can be formalised as follows:

$$I_p = D_s(I_{low}), \tag{14}$$

where I_{low} is a low-light image. By constraining the reconstruction loss to this weighted combination, the network adaptively suppresses unreliable components during end-to-end training. The LLIE task can be formalised as follows:

$$\arg\min_{\varepsilon} Loss = (\mathcal{F}_{net\varepsilon}(I_p \cdot I_{low}), I_{nomal}), \tag{15}$$

where I_{low} is a low-light image, I_{normal} is a normal light image, loss is the loss function of the network and $\mathcal{F}_{net\varepsilon}$ is the network with parameter ε.

5 Experiments

5.1 Experimental Settings

To verify the effectiveness of the proposed method, we compare different public datasets with classical and advanced methods for classification and low-light image enhancement (LLIE). The publicly available datasets include CIFAR-10 (Ganjdanesh et al., 2024), MNIST (Li et al., 2025), Fashion-MNIST (Yang et al., 2024), LOL-v1 (Cai et al., 2023), LOL-v2-real (Yang et al., 2021), LOL-v2-syn(Fan et al., 2025b), Iris (Veenman & Reinders, 2005), Heart (Xu et al., 2016), Hepatitis (Xu et al., 2013), Parkinson's (Little, 2007), Australian (Xiao et al., 2023), and five datasets without unavailable ground truth, namely, NPE (Wang et al., 2013), DICM (Lee et al., 2013), MEF (Ma et al., 2015), LIME (Guo et al., 2017), and VV (Vonikakis et al., 2018). The experimental results were evaluated by the accuracy (ACC), the peak signal-to-noise ratio (PSNR) (Winkler & Mohandas, 2008), and structural similarity (SSIM) (Wang et al., 2004). Moreover, the natural image quality evaluator (NIQE) (Zhang et al., 2015), and the perceptual index (PI) (Fan et al., 2025b) serve as metrics for evaluating experiments on datasets lacking ground truth data. The parameters (Param) and floating point operations (FLOPs) are used to measure model complexity. We propose a method that is implemented in the PyTorch framework and trained by the AdamW optimiser, with initial learning rates of 10^{-4} and exponential decay rates of 0.9 and 0.999, respectively.

5.2 Numerical Experiment of DNBBA

Let $\Phi = \{w_1, w_2, w_3\}$, $m(w_1) = 0.65$, $m(w_2) = 0.1$, and $m(w_3) = 0.25$. The variation in the negative v iteration is shown in Figure 2a, which shows that as the number of negation iterations increases, $\bar{m}_v\ (w_i)$ gradually converges when the BBA contains only a single element. We used aggregated uncertainty (AU) (Yin et al., 2019), the ambiguity measure (AM) (Yin et al., 2019), the confusion measure (Conf) (Yin et al., 2019), the dissonance measure (Diss) (Yager, 2008), and measures for specificity (NS) (Yager, 2008) for the uncertainty measure under the v iteration of negation. The results are shown in Figure 2b, which reveals that the uncertainty of the system reaches

its maximum when the confidence distribution tends to be uniform, whereas the NS value remains zero because it focuses only on focal elements with large cardinality. Combining the results of Figure 2a and Figure 2b intuitively verifies that the DNBBA method tends to be uniformly distributed after several iterations, and the system uncertainty tends to be stable with iteration convergence.

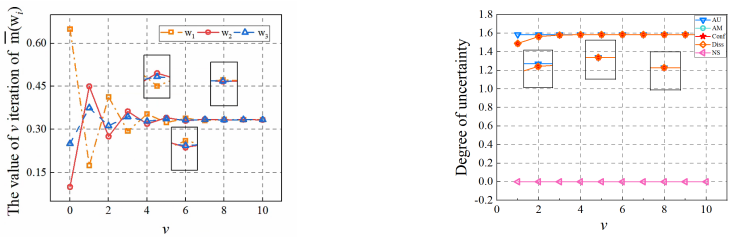

(a) (b)

Figure 2: Illustration of the change in v iteration of negation. (a) Value of the v iteration of $\bar{m}$ (w_i). (b) The degree of uncertainty of v iteration of negation under five different measures.

5.3 Pattern Classification

We used the same test method as Xiao et al. (2023), divided the training set and the test set according to a 4:1 ratio, obtained the results of fivefold cross-validation, and then averaged these results as the final result. In Table 1, the experimental results show that our proposed method achieves the best accuracy (ACC) on Iris, Heart, Hepatitis, Parkinson's and Australian in terms of classification accuracy evaluation indicators, which are 2%, 6.08%, 2.84%, 1.84% and 2.39% higher than those of the advanced DMA method, respectively. These findings indicate that DNBBA-DNet can more effectively utilise evidence theory to optimise classification decisions when dealing with datasets with different features and class distributions, which improves the accuracy and robustness of classification.

5.4 Image Classification

We selected efficient channel attention for deep convolutional neural networks (Wang et al., 2020) as the backbone network for image feature extraction and conducted a comparative analysis of image classification with advanced methods on different public datasets. As illustrated in Table 2, the experimental results show that our proposed method achieves the best accuracy on CIFAR-10, MNIST and Fashion-MNIST, and the proposed method is 1.27%, 0.71% and 1.87% better than the state-of-the-art methods, respectively. These results show that DNBBA-DNet has excellent performance in image classification tasks and can verify the effectiveness of DNBBA.

Table 1: Accuracy of different methods on Iris, Heart, Hepatitis, Parkinson's, and Australian (%). The best, second and third results are in the red, green and blue colors.

Methods	Iris	Heart	Hepatitis	Parkinson's	Australian
kNN (Cover & Hart, 1967)	95.33	57.78	65.71	83.02	67.40
RBFN (CHEN S & Grant, 1991)	92.67	81.85	81.32	82.05	82.61
kNN-DST (Denoeux, 1995)	95.33	76.30	80.57	78.01	78.41
REPTree (Freund & Mason, 1999)	92.00	70.74	71.64	80.94	80.59
NMC (Veenman & Reinders, 2005)	90.67	60.37	52.14	70.77	64.21
SVM (Chang & Lin, 2011)	94.67	83.70	79.96	70.13	80.29
CSMlP (Castro & Braga, 2013)	93.33	75.19	74.93	74.39	82.32
NDC (Xu et al., 2013)	94.00	82.59	79.40	70.26	80.01
EvC (Xu et al., 2016)	94.67	83.70	79.88	81.64	80.60
DMA (Xiao et al., 2023)	96.00	84.07	83.04	75.03	84.14
DNBBA-DNet	98.00	90.15	85.88	84.86	86.53

5.5 Low-light Image Enhancement

In LLIE, dark regions often contain crucial information. However, traditional training strategies uniformly process the entire image, making it difficult for models to fully learn these critical areas and resulting in poor detail recovery in target regions. To address this, we propose a method based

Table 2: Accuracy of different methods on CIFAR-10, MNIST, and Fashion-MNIST (%). The best, second and third results are in the red, green and blue colors.

	Methods	ACC	Methods	ACC	Methods	ACC
CIFAR-10	IGEBM (Du & Mordatch, 2019)	49.10	LWC (Han et al., 2015)	98.40	FREM (Zhang et al., 2018)	93.80
	GDAS (Dong & Yang, 2019)	92.60	DNS (Guo et al., 2016)	98.00	Efficientne (Tan & Le, 2019)	93.64
	JEM (Grathwohl et al., 2020)	93.70	SWS (Ullrich et al., 2017)	98.10	CNN+HPO+Reg (Greeshma & Sreekumar, 2019)	93.99
	Dspike (Li et al., 2021)	94.25	LC (Carreira-Perpinan & Idelbayev, 2018)	96.80	DCN-UN (Chen & Liu, 2020)	93.68
	DSC (Zheng et al., 2021)	88.29	SNIP (Lee et al., 2019)	97.60	VIT (Dosovitskiy et al., 2020)	90.98
	GLIF (Yao et al., 2022)	94.15	ProsPr (Alizadeh et al., 2022)	97.20	VGG Network (Duan et al., 2019)	91.50
	RF-DARTS (Zhang et al., 2023)	94.42	TEDEPR (Liu et al., 2024)	98.00	SCNN (Zhang et al., 2022a)	92.60
	UDSP (Gao et al., 2024)	93.78	MPIS-SNNs (Cao et al., 2024)	99.05	MCNN15 (Nocentini et al., 2022)	94.04
	SOL (Song et al., 2024)	93.57	M-BLS (Wang et al., 2025)	99.08	MPIS-SNNs (Cao et al., 2024)	93.36
	RLAL (Ganjdanesh et al., 2024)	94.85	MC-MSLs RC (Li et al., 2025)	99.11	RT-ECN (Zhou et al., 2025)	93.42
	DNBBA-DNet	96.12	DNBBA-DNet	99.82	DNBBA-DNet	95.91

MNIST

Fashion-MNIST

on $\mathcal{F}_{net\varepsilon}$ (Cai et al., 2023) that explicitly guides the model to enhance its attention to regions with high degradation levels. From the experimental results in Table 3, our method performs well on the low-light image enhancement task. For the LOL-v1, LOL-v2-real and LOL-v2-syn datasets, our method achieves PSNR values of 24.75, 22.46 and 26.19, respectively, and SSIM values of 0.899, 0.901 and 0.946, respectively, which are mostly better than those of the other comparison methods. The visualisation results in Figure 3 demonstrate that in the first row, our method enhances the

Table 3: Quantitative comparison of LOL-v1, LOL-v2-real, and LOL-v2-syn. The best, second and third results are in the red, green and blue colors.

Methods	LOL-v1		LOL-v2-real		LOL-v2-syn	
	PSNR	SSIM	PSNR	SSIM	PSNR	SSIM
Sparse (Yang et al., 2021)	17.20	0.640	20.06	0.816	22.05	0.905
3DLUT (Zeng et al., 2022)	14.35	0.445	17.59	0.721	18.04	0.800
ZeroDCE++ (Li et al., 2022b)	16.11	0.530	18.06	0.577	18.03	0.825
SCI (Ma et al., 2022)	14.78	0.525	16.19	0.522	16.67	0.811
UFormer (Wang et al., 2022)	16.36	0.771	18.82	0.771	19.66	0.871
SNR (Xu et al., 2022)	24.61	0.842	21.48	0.849	24.14	0.928
Restormer (Jiang et al., 2023)	22.43	0.823	19.94	0.827	21.41	0.830
Retinexforme r(Cai et al., 2023)	25.16	0.845	22.80	0.840	25.67	0.930
CIDNet (Yan et al., 2025)	23.50	0.870	23.43	0.862	25.71	0.942
Ours	24.75	0.899	22.46	0.901	26.19	0.946

texture of the clothing in the magnified area, whereas in the second and third rows, it corrects color casts in the sky and wall surfaces. In addition, we have expanded cross-database experiments across five datasets. We employed the optimal model trained on LOL-v2-syn to evaluate various methods, as presented in Table 4. The results demonstrate that our method achieves favourable PI alongside favourable NIQE and indicate that introducing DNBBA increases model complexity. However, considering the improvement in model performance, this increase remains within acceptable limits, which proves the actual application efficiency of our method.

Table 4: Quantitative comparison of cross-database. The best, second and third results are in red, green and blue colors.

Methods	Complexity		NPE		DICM		MEF		LIME		VV	
	Param (M)	FLOPs (G)	NIQE	PI	NIQE	PI	NIQE	PI	NIQE	PI	NIQE	PI
Uformer (Wang et al., 2022)	5.29	12.00	3.393	2.7740	3.147	3.1426	3.207	2.6219	3.627	2.8206	2.557	2.6228
SNR (Xu et al., 2022)	4.01	26.35	3.151	3.6195	3.287	4.5940	3.071	3.5144	4.570	4.5590	4.274	6.1386
Restormer (Jiang et al., 2023)	26.13	144.25	3.420	2.8011	2.966	3.1529	3.115	2.6157	3.849	2.8796	2.566	2.6771
Retinexformer (Cai et al., 2023)	1.61	15.57	4.254	2.8524	3.732	3.0831	3.881	2.7133	4.002	2.9623	3.270	2.7821
CIDNet (Yan et al., 2025)	1.88	7.57	3.741	2.8042	3.787	3.1530	3.560	2.5837	4.130	3.0438	3.211	3.4740
Ours	2.17	21.65	3.252	2.6551	3.170	3.0129	3.033	2.5068	3.686	2.8057	3.050	2.5513

5.6 Ablation Study

To validate the necessity of our proposed module, we conducted ablation experiments using three datasets. As shown in Table 5, compared with the baseline method, the introduction of the BBA



Figure 3: Qualitative comparison of LOL-v1 (Cai et al., 2023) (1st row), LOL-v2-real (Yang et al., 2021) (2nd row), and LOL-v2-syn (Yang et al., 2021) (3rd row).

module improved accuracy across the three datasets, confirming the essential role of the BBA module in enhancing baseline performance. Furthermore, the accuracy achieved by the models built solely with BBA did not surpass that of the models incorporating DNBBA across all three datasets, which indicates that DNBBA compensates for the limitations of traditional DST methods, which focus solely on positive evidence accumulation. Moreover, to validate the effectiveness of ρ, we

Table 5: Accuracy of different components (%).

Methods	CIFAR-10	MNIST	Fashion-MNIST
baseline (Wang et al., 2020)	93.25	98.15	93.31
+BBA	94.97	99.03	94.17
+DNBBA ($w/\ \rho$)	**96.12**	**99.82**	**95.91**

constructed three datasets based on partial label learning (PLL) (Huang et al., 2025a), including CIFAR-10+PLL (CPLL), MNIST+PLL (MPLL), and Fashion-MNIST+PLL (FPLL). As shown in Table 6, the results demonstrate that the method incorporating the learnable parameter ρ achieves optimal performance across all three datasets, confirming that ρ effectively enhances model performance under multisource focal elements.

Table 6: Accuracy of different components on the CPLL, MPLL, and FPLL (%).

Methods	CPLL	MPLL	FPLL
baseline (Wang et al., 2020)	66.75	77.85	68.45
+BBA	78.53	86.12	79.72
+DNBBA ($w/o\ \rho$)	82.21	86.99	81.24
+DNBBA ($\rho = 3$)	82.75	87.01	81.83
+DNBBA ($w/\ \rho$)	**83.31**	**87.82**	**82.76**

6 Conclusion

In this paper, we propose a method based on DNBBA, which aims to achieve the bidirectional dynamic revision of beliefs by simultaneously measuring the strength of support and refutation to improve decision and classification performance. By constructing a learnable asymmetric similarity function, the DNBBA overcomes the limitations of traditional DST, which relies only on positive evidence, and effectively alleviates the decision bias caused by class imbalance and evidence conflict. DNBBA-DNet is further proposed to uniformly optimise the classification and low-light image enhancement tasks by minimising the negative belief criterion. The experimental results show that the proposed method is superior to the existing mainstream algorithms on multiple benchmark datasets and improves the classification accuracy and overall performance of low-light image enhancement.

AI USE STATEMENT

In this work, we used generative AI tools for assisting with minor code implementation and debugging. We have not used generative AI tools for developing the core research ideas, designing the proposed methodology, conducting experiments, analyzing experimental results, or generating the scientific claims presented in this work. We have reviewed all AI-assisted work. The AI-assisted code was manually verified and tested by 2 authors to ensure its correctness. We take responsibility for the final content of this work, including text, claims, and artifacts produced with the aid of generative AI.

REPRODUCIBILITY STATEMENT

We have made efforts to ensure the reproducibility of our work. Detailed experimental configurations, implementation details, and additional results are provided in the Appendix. The theoretical analysis and complete proofs of the claims are also included in the Appendix. In addition, we release anonymous source code at `https://anonymous.4open.science/r/DNBBA-DNet` as supplementary material, which contains the implementation of our proposed method.

REFERENCES

Milad Alizadeh, Shyam A Tailor, Luisa M Zintgraf, Joost Van Amersfoort, Sebastian Farquhar, Nicholas Donald Lane, and Yarin Gal. Prospect pruning: Finding trainable weights at initialization using meta-gradients. In *International Conference on Learning Representations*, 2022.

Ayyub Alzahem, Wadii Boulila, Maha Driss, and Anis Koubaa. Feature fusion for improved classification: combining dempster-shafer theory and multiple cnn architectures. In *International Conference on Computational Collective Intelligence*, pp. 280–292. Springer, 2024.

Yuanhao Cai, Hao Bian, Jing Lin, Haoqian Wang, Radu Timofte, and Yulun Zhang. Retinexformer: One-stage Retinex-based Transformer for Low-light Image Enhancement . In *2023 IEEE/CVF International Conference on Computer Vision (ICCV)*, pp. 12470–12479, Los Alamitos, CA, USA, October 2023. IEEE Computer Society. doi: 10.1109/ICCV51070.2023.01149.

Zhigao Cao, Meng Li, Xiashuang Wang, Haoyu Wang, Fan Wang, Youjun Li, and Zi-Gang Huang. Efficient training of spiking neural networks with multi-parallel implicit stream architecture. In *European Conference on Computer Vision*, pp. 422–438. Springer, 2024.

Miguel A. Carreira-Perpinan and Yerlan Idelbayev. "learning-compression" algorithms for neural net pruning. In *2018 IEEE/CVF Conference on Computer Vision and Pattern Recognition (CVPR)*, pp. 8532–8541, 2018. doi: 10.1109/CVPR.2018.00890.

Cristiano L. Castro and Antônio P. Braga. Novel cost-sensitive approach to improve the multilayer perceptron performance on imbalanced data. *IEEE Transactions on Neural Networks and Learning Systems*, 24(6):888–899, 2013. doi: 10.1109/TNNLS.2013.2246188.

Chih Chung Chang and Chih Jen Lin. Libsvm: a library for support vector machines. *ACM transactions on intelligent systems and technology (TIST)*, 2(3):1–27, 2011.

Junying Chen and Zhan Liu. Mask dynamic routing to combined model of deep capsule network and u-net. *IEEE Transactions on Neural Networks and Learning Systems*, 31(7):2653–2664, 2020. doi: 10.1109/TNNLS.2020.2984686.

Grant Merle CHEN S and PM Grant. Orthogonal least squares learning algorithm for radial basis function networks. *IEEE Transactions on Neural Networks*, 2(2):302–309, 1991.

Thomas Cover and Peter Hart. Nearest neighbor pattern classification. *IEEE transactions on information theory*, 13(1):21–27, 1967.

T. Denoeux. A k-nearest neighbor classification rule based on dempster-shafer theory. *IEEE Transactions on Systems, Man, and Cybernetics*, 25(5):804–813, 1995. doi: 10.1109/21.376493.

Xuanyi Dong and Yi Yang. Searching for a robust neural architecture in four gpu hours. In *2019 IEEE/CVF Conference on Computer Vision and Pattern Recognition (CVPR)*, pp. 1761–1770, 2019. doi: 10.1109/CVPR.2019.00186.

Alexey Dosovitskiy, Lucas Beyer, Alexander Kolesnikov, Dirk Weissenborn, Xiaohua Zhai, Thomas Unterthiner, Mostafa Dehghani, Matthias Minderer, G Heigold, S Gelly, et al. An image is worth 16x16 words: Transformers for image recognition at scale. In *International Conference on Learning Representations*, 2020.

Yilun Du and Igor Mordatch. Implicit generation and modeling with energy based models. *Advances in neural information processing systems*, 32, 2019.

Chao Duan, Panpan Yin, Yan Zhi, and Xingxing Li. Image classification of fashion-mnist data set based on vgg network. In *Proceedings of 2019 2nd International Conference on Information Science and Electronic Technology (ISET 2019). International Informatization and Engineering Associations: Computer Science and Electronic Technology International Society*, volume 19, 2019.

Linlin Fan, Xingyu Liu, Mingliang Zhou, Xuekai Wei, Weizhi Xian, Jielu Yan, and Weijia Jia. A dynamic learning strategy for dempster-shafer theory with applications in classification and enhancement. In D. Belgrave, C. Zhang, H. Lin, R. Pascanu, P. Koniusz, M. Ghassemi, and N. Chen (eds.), *Advances in Neural Information Processing Systems*, volume 38, pp. 12215–12242. Curran Associates, Inc., 2025a.

Linlin Fan, Xuekai Wei, Mingliang Zhou, Jielu Yan, Huayan Pu, Jun Luo, and Zhengguo Li. A semantic-aware detail adaptive network for image enhancement. *IEEE Transactions on Circuits and Systems for Video Technology*, 35(2):1787–1800, 2025b. doi: 10.1109/TCSVT.2024.3483191.

Yoav Freund and Llew Mason. The alternating decision tree learning algorithm. In *Proceedings of the Sixteenth International Conference on Machine Learning*, ICML '99, pp. 124–133, San Francisco, CA, USA, 1999. Morgan Kaufmann Publishers Inc. ISBN 1558606122.

Alireza Ganjdanesh, Shangqian Gao, and Heng Huang. Jointly training and pruning cnns via learnable agent guidance and alignment. In *2024 IEEE/CVF Conference on Computer Vision and Pattern Recognition (CVPR)*, pp. 16058–16069, 2024. doi: 10.1109/CVPR52733.2024.01520.

Shangqian Gao, Yanfu Zhang, Feihu Huang, and Heng Huang. Bilevelpruning: Unified dynamic and static channel pruning for convolutional neural networks. In *2024 IEEE/CVF Conference on Computer Vision and Pattern Recognition (CVPR)*, pp. 16090–16100, 2024. doi: 10.1109/CVPR52733.2024.01523.

Will Grathwohl, Kuan-Chieh Wang, Jörn-Henrik Jacobsen, David Duvenaud, Mohammad Norouzi, and Kevin Swersky. Your classifier is secretly an energy based model and you should treat it like one. In *International Conference on Learning Representations*, 2020.

KV Greeshma and K Sreekumar. Hyperparameter optimization and regularization on fashion-mnist classification. *International Journal of Recent Technology and Engineering (IJRTE)*, 8(2):3713–3719, 2019.

Xiaojie Guo, Yu Li, and Haibin Ling. Lime: Low-light image enhancement via illumination map estimation. *IEEE Transactions on Image Processing*, 26(2):982–993, 2017. doi: 10.1109/TIP.2016.2639450.

Yiwen Guo, Anbang Yao, and Yurong Chen. Dynamic network surgery for efficient dnns. *Advances in neural information processing systems*, 29, 2016.

Song Han, Jeff Pool, John Tran, and William Dally. Learning both weights and connections for efficient neural network. *Advances in neural information processing systems*, 28, 2015.

Ke He, Deqiang Han, and Xiaojing others Fan. Learning-based bba modeling method with attribute interval number. In *2021 International Conference on Control, Automation and Information Sciences (ICCAIS)*, pp. 931–935, 2021. doi: 10.1109/ICCAIS52680.2021.9624594.

Jintao Huang, Yiu-ming Cheung, Chi-man Vong, and Wenbin Qian. Gbrip: Granular ball representation for imbalanced partial label learning. In *Proceedings of the AAAI Conference on Artificial Intelligence*, volume 39, pp. 17431–17439, 2025a.

Yingcheng Huang, Fuyuan Xiao, Zehong Cao, and Chin-Teng Lin. Fractal belief rényi divergence with its applications in pattern classification. *IEEE Transactions on Knowledge and Data Engineering*, 36(12):8297–8312, 2024. doi: 10.1109/TKDE.2023.3342907.

Yueting Huang, Zhenzhe Hechen, Mingliang Zhou, et al. An attention-locating algorithm for eliminating background effects in fine-grained visual classification. *IEEE Transactions on Circuits and Systems for Video Technology*, pp. 1–1, 2025b. doi: 10.1109/TCSVT.2025.3535818.

Nanfeng Jiang, Junhong Lin, Ting Zhang, Haifeng Zheng, and Tiesong Zhao. Low-light image enhancement via stage-transformer-guided network. *IEEE Transactions on Circuits and Systems for Video Technology*, 33(8):3701–3712, 2023. doi: 10.1109/TCSVT.2023.3239511.

Chulwoo Lee, Chul Lee, and Chang-Su Kim. Contrast enhancement based on layered difference representation of 2d histograms. *IEEE transactions on image processing*, 22(12):5372–5384, 2013.

N Lee, T Ajanthan, and P Torr. Snip: single-shot network pruning based on connection sensitivity. In *International Conference on Learning Representations*. Open Review, 2019.

Bolian Li, Zongbo Han, Haining Li, Huazhu Fu, and Changqing Zhang. Trustworthy long-tailed classification. In *2022 IEEE/CVF Conference on Computer Vision and Pattern Recognition (CVPR)*, pp. 6960–6969, 2022a. doi: 10.1109/CVPR52688.2022.00684.

Chongyi Li, Chunle Guo, and Chen Change Loy. Learning to enhance low-light image via zero-reference deep curve estimation. *IEEE Transactions on Pattern Analysis and Machine Intelligence*, 44(8):4225–4238, 2022b. doi: 10.1109/TPAMI.2021.3063604.

Shuxian Li, Liyan Song, Xiaoyu Wu, Zheng Hu, Yiu-ming Cheung, and Xin Yao. Multi-class imbalance classification based on data distribution and adaptive weights. *IEEE Transactions on Knowledge and Data Engineering*, 36(10):5265–5279, 2024a.

Siyuan Li, Deqiang Han, and Jean others Dezert. Learning-based bba modeling approach with multi-method fusion. In *2024 27th International Conference on Information Fusion (FUSION)*, pp. 1–6, 2024b. doi: 10.23919/FUSION59988.2024.10706437.

Yanshu Li, Bohan Hu, Zhengdao Li, Linshan Li, Weiming Liu, Ruizhi Qian, Guangxin Wu, Hao Zhang, Jifeng Shen, Piotr Koniusz, et al. Deco-detr: Decoupled cognition detr for efficient open-vocabulary object detection. In *International Conference on Learning Representations*, volume 2026, pp. 124043–124063, 2026.

Yuhang Li, Yufei Guo, Shanghang Zhang, Shikuang Deng, Yongqing Hai, and Shi Gu. Differentiable spike: Rethinking gradient-descent for training spiking neural networks. *Advances in neural information processing systems*, 34:23426–23439, 2021.

Zelin Li, Yiyuan Xie, Fang Xu, Yichen Ye, Xiao Jiang, Ye Su, Lili Li, Zhuang Chen, and Yuhan Tang. Time-delayed reservoir computing using mutually coupled multimode semiconductor laser for high-speed image recognition. *Optics Laser Technology*, 187:112774, 2025. ISSN 0030-3992. doi: https://doi.org/10.1016/j.optlastec.2025.112774.

Max Little. Parkinsons. UCI Machine Learning Repository, 2007. DOI: https://doi.org/10.24432/C59C74.

An Liu, Yufan Zhou, and Wenkang Xu. Subspace constrained variational bayesian inference for structured compressive sensing with a dynamic grid. *IEEE Transactions on Signal Processing*, 73:781–794, 2025. doi: 10.1109/TSP.2025.3532953.

Debin Liu, Xiang Bai, Ruonan Zhao, Xianjun Deng, and Laurence T. Yang. Dual-grained lightweight strategy. *IEEE Transactions on Pattern Analysis and Machine Intelligence*, 46(12): 10228–10245, 2024. doi: 10.1109/TPAMI.2024.3437421.

Kede Ma, Kai Zeng, and Zhou Wang. Perceptual quality assessment for multi-exposure image fusion. *IEEE Transactions on Image Processing*, 24(11):3345–3356, 2015. doi: 10.1109/TIP.2015.2442920.

Long Ma, Tengyu Ma, Risheng Liu, Xin Fan, and Zhongxuan Luo. Toward fast, flexible, and robust low-light image enhancement. In *2022 IEEE/CVF Conference on Computer Vision and Pattern Recognition (CVPR)*, pp. 5627–5636, 2022. doi: 10.1109/CVPR52688.2022.00555.

Olivia Nocentini, Jaeseok Kim, Muhammad Zain Bashir, and Filippo Cavallo. Image classification using multiple convolutional neural networks on the fashion-mnist dataset. *Sensors*, 22(23):9544, 2022.

Jinseong Park, Yujin Choi, and Jaewook Lee. In-distribution public data synthesis with diffusion models for differentially private image classification. In *2024 IEEE/CVF Conference on Computer Vision and Pattern Recognition (CVPR)*, pp. 12236–12246, 2024. doi: 10.1109/CVPR52733.2024.01163.

Pratibha Rani, Shyi-Ming Chen, and Arunodaya Raj Mishra. Multi-attribute decision-making based on similarity measure between picture fuzzy sets and the marcos method. *Information Sciences*, 658:119990, 2024.

Xiaotian Song, Peng Zeng, Yanan Sun, and Andy Song. Generalizable symbolic optimizer learning. In *European Conference on Computer Vision*, pp. 36–52. Springer, 2024.

Rui Sun, Yiwen Yang, Kaiyu Guo, Chen Jiang, Dongli Xu, Zhaonan Liu, Tan Pan, LIMEI HAN, Xue Jiang, Wu Wei, and Yuan Cheng. Disco: Densely-overlapping cell instance segmentation via adjacency-aware collaborative coloring. In *The Fourteenth International Conference on Learning Representations*, 2026.

Mingxing Tan and Quoc Le. Efficientnet: Rethinking model scaling for convolutional neural networks. In *International conference on machine learning*, pp. 6105–6114. PMLR, 2019.

Karen Ullrich, Edward Meeds, and Max Welling. Soft weight-sharing for neural network compression. In *International Conference on Learning Representations*, 2017.

Cor J Veenman and Marcel JT Reinders. The nearest subclass classifier: A compromise between the nearest mean and nearest neighbor classifier. *IEEE Transactions on Pattern Analysis and Machine Intelligence*, 27(9):1417–1429, 2005.

Vassilios Vonikakis, Rigas Kouskouridas, and Antonios Gasteratos. On the evaluation of illumination compensation algorithms. *Multimedia Tools and Applications*, 77(8):9211–9231, 2018.

Jing Wang, Luyu Nie, Junwei Duan, Huimin Zhao, and C. L. Philip Chen. Mixture-of-experts-based broad learning system and its applications. *Expert Systems with Applications*, 269:126389, 2025. ISSN 0957-4174. doi: https://doi.org/10.1016/j.eswa.2025.126389.

Qilong Wang, Banggu Wu, Pengfei Zhu, Peihua Li, Wangmeng Zuo, and Qinghua Hu. Eca-net: Efficient channel attention for deep convolutional neural networks. pp. 11534–11542, 2020.

Shuhang Wang, Jin Zheng, Hai-Miao Hu, and Bo Li. Naturalness preserved enhancement algorithm for non-uniform illumination images. *IEEE Transactions on Image Processing*, 22(9):3538–3548, 2013. doi: 10.1109/TIP.2013.2261309.

Zhendong Wang, Xiaodong Cun, Jianmin Bao, Wengang Zhou, Jianzhuang Liu, and Houqiang Li. Uformer: A general u-shaped transformer for image restoration. In *2022 IEEE/CVF Conference on Computer Vision and Pattern Recognition (CVPR)*, pp. 17662–17672, 2022. doi: 10.1109/CVPR52688.2022.01716.

Zhou Wang, Alan C Bovik, Hamid R Sheikh, and Eero P Simoncelli. Image quality assessment: from error visibility to structural similarity. *IEEE transactions on image processing*, 13(4):600–612, 2004.

Stefan Winkler and Praveen Mohandas. The evolution of video quality measurement: From psnr to hybrid metrics. *IEEE transactions on Broadcasting*, 54(3):660–668, 2008.

Fuyuan Xiao. Generalization of dempster-shafer theory: A complex mass function. *Applied Intelligence*, 50:3266–3275, 2020.

Fuyuan Xiao, Junhao Wen, and Witold Pedrycz. Generalized divergence-based decision making method with an application to pattern classification. *IEEE Transactions on Knowledge and Data Engineering*, 35(7):6941–6956, 2023. doi: 10.1109/TKDE.2022.3177896.

Fuyuan Xiao, Weiping Ding, and Witold Pedrycz. A generalized ff-divergence with applications in pattern classification. *IEEE Transactions on Knowledge and Data Engineering*, 37(4):1556–1570, 2025. doi: 10.1109/TKDE.2025.3530524.

Peida Xu, Yong Deng, Xiaoyan Su, and Sankaran Mahadevan. A new method to determine basic probability assignment from training data. *Knowledge-Based Systems*, 46:69–80, 2013. ISSN 0950-7051. doi: https://doi.org/10.1016/j.knosys.2013.03.005.

Philippe Xu, Franck Davoine, Hongbin Zha, and Thierry Denœux. Evidential calibration of binary svm classifiers. *International Journal of Approximate Reasoning*, 72:55–70, 2016. ISSN 0888-613X. doi: https://doi.org/10.1016/j.ijar.2015.05.002. BELIEF 2014 – Third International Conference on Belief Functions.

Xiaogang Xu, Ruixing Wang, Chi-Wing Fu, and Jiaya Jia. Snr-aware low-light image enhancement. In *2022 IEEE/CVF Conference on Computer Vision and Pattern Recognition (CVPR)*, pp. 17693–17703, 2022. doi: 10.1109/CVPR52688.2022.01719.

Ronald R. Yager. *Entropy and Specificity in a Mathematical Theory of Evidence*, pp. 291–310. Springer Berlin Heidelberg, Berlin, Heidelberg, 2008. ISBN 978-3-540-44792-4. doi: 10.1007/978-3-540-44792-4_11.

Qingsen Yan, Yixu Feng, Cheng Zhang, Guansong Pang, Kangbiao Shi, Peng Wu, Wei Dong, Jinqiu Sun, and Yanning Zhang. Hvi: A new color space for low-light image enhancement. In *Proceedings of the Computer Vision and Pattern Recognition Conference*, pp. 5678–5687, 2025.

Wenhan Yang, Wenjing Wang, Haofeng Huang, Shiqi Wang, and Jiaying Liu. Sparse gradient regularized deep retinex network for robust low-light image enhancement. *IEEE Transactions on Image Processing*, 30:2072–2086, 2021. doi: 10.1109/TIP.2021.3050850.

Yuxuan Yang, Zihao Xuan, and Yi Kang. Tq-ttfs: High-accuracy and energy-efficient spiking neural networks using temporal quantization time-to-first-spike neuron. In *2024 29th Asia and South Pacific Design Automation Conference (ASP-DAC)*, pp. 836–841, 2024. doi: 10.1109/ASP-DAC58780.2024.10473964.

Xingting Yao, Fanrong Li, Zitao Mo, and Jian Cheng. Glif: A unified gated leaky integrate-and-fire neuron for spiking neural networks. *Advances in Neural Information Processing Systems*, 35: 32160–32171, 2022.

Kai Ye, Tiejin Chen, Hua Wei, and Liang Zhan. Uncertainty regularized evidential regression. In *Proceedings of the AAAI Conference on Artificial Intelligence*, volume 38, pp. 16460–16468, 2024.

Likang Yin, Xinyang Deng, and Yong Deng. The negation of a basic probability assignment. *IEEE Transactions on Fuzzy Systems*, 27(1):135–143, 2019. doi: 10.1109/TFUZZ.2018.2871756.

Hui Zeng, Jianrui Cai, Lida Li, Zisheng Cao, and Lei Zhang. Learning image-adaptive 3d lookup tables for high performance photo enhancement in real-time. *IEEE Transactions on Pattern Analysis and Machine Intelligence*, 44(4):2058–2073, 2022. doi: 10.1109/TPAMI.2020.3026740.

Anguo Zhang, Xiumin Li, Yueming Gao, and Yuzhen Niu. Event-driven intrinsic plasticity for spiking convolutional neural networks. *IEEE Transactions on Neural Networks and Learning Systems*, 33(5):1986–1995, 2022a. doi: 10.1109/TNNLS.2021.3084955.

Lin Zhang, Lei Zhang, and Alan C Bovik. A feature-enriched completely blind image quality evaluator. *IEEE Transactions on Image Processing*, 24(8):2579–2591, 2015.

Suofei Zhang, Quan Zhou, and Xiaofu Wu. Fast dynamic routing based on weighted kernel density estimation. In *International symposium on artificial intelligence and robotics*, pp. 301–309. Springer, 2018.

Xuanyang Zhang, Yonggang Li, Xiangyu Zhang, Yongtao Wang, and Jian Sun. Differentiable architecture search with random features. In *2023 IEEE/CVF Conference on Computer Vision and Pattern Recognition (CVPR)*, pp. 16060–16069, 2023. doi: 10.1109/CVPR52729.2023.01541.

Zuo Wei Zhang, Zhe Liu, Zong Fang Ma, Yiru Zhang, and Hao Wang. A new belief-based incomplete pattern unsupervised classification method. *IEEE Transactions on Knowledge and Data Engineering*, 34(11):5084–5097, 2022b. doi: 10.1109/TKDE.2021.3049511.

Tong Zheng, Xu Philippe, and Denœux Thierry. An evidential classifier based on dempster-shafer theory and deep learning. *Neurocomputing*, 450:275–293, 2021. ISSN 0925-2312.

Minghao Zhou, Shuxian Lun, and Ming Li. Rapid training echo convolution network for image recognition. *Information Sciences*, 696:121750, 2025. ISSN 0020-0255. doi: https://doi.org/10.1016/j.ins.2024.121750.

A Appendix

A.1 Dempster's rule of combination

Let m_1 and m_2 are two independent basic belief assignments (BBAs) with propositions τ_k and τ_i in FOD Θ. Dempster's rule of combination, denoted as $m = m_1 \oplus m_2$, is defined as follows:

$$m(\tau) = \begin{cases} \frac{\sum_{\tau_k \cap \tau_i = \tau} m_1(\tau_k) m_2(\tau_i)}{1-\mathrm{K}}, & \tau \neq \emptyset, \\ 0, & \tau = \emptyset, \end{cases} \tag{16}$$

with

$$\mathrm{K} = \sum_{\tau_k \cap \tau_i = \emptyset} m_1(\tau_k) m_2(\tau_i), \tag{17}$$

where K is the conflict coefficient between $m_1(\tau_k)$ and $m_2(\tau_i)$. $\tau_k \in 2^\Theta$ and $\tau_i \in 2^\Theta$.

A.2 More Proof Details for Theorems and Properties

This subsection presents the DNBBA as well as its theorems, properties, corollaries, and proofs. Θ is a set of mutually exclusive events, and L_ξ is a nonempty event .
Let m be a BBA on $\Theta = \{L_1, L_2, \cdots, L_\xi\}$. The dynamic negation of basic belief assignment is defined as follows:

$$\bar{m}\left(\tau_i\right) = \sum_{\tau_k \subset \Theta} m(\tau_k) \cdot \psi(\tau_i, \tau_k), \tag{18}$$

with

$$\psi(\tau_i, \tau_k) = \frac{\bar{\psi}\left(\tau_i, \tau_k\right)}{\sum_{\tau_i \subset \Theta} \bar{\psi}\left(\tau_i, \tau_k\right)}, \tag{19}$$

$$\bar{\psi}\left(\tau_i, \tau_k\right) = \alpha \cdot \frac{|\tau_i \backslash \tau_k|}{|\tau_i|} + \beta \cdot \frac{|\tau_k \backslash \tau_i|}{|\tau_k|}, \tag{20}$$

and satisfies

$$\begin{aligned} \alpha = \exp\left(-\rho \cdot |m(\tau_i) - m(\tau_k)|\right), \\ \alpha + \beta = 1, \\ \bar{m}\left(\emptyset\right) = 1, \end{aligned} \tag{21}$$

where ρ is the smooth attenuation coefficient and where $|\cdot|$ is the cardinality.
Property 1. The function is nonnegative. $\forall \tau_i, \tau_k, \psi(\tau_i, \tau_k) \geq 0$ and $m(\tau_k) \geq 0$, from which we can

derive $\bar{m}\ (\tau_i) \geq 0$.

Theorem 1. When $|\tau_i| = 1, \tau_i \cap \tau_k = \emptyset$, the mathematical expression for $\bar{m}\ (\tau_i)$ is as follows:

$$\begin{aligned} \bar{m}\ (\tau_i) &= \frac{\sum_{\tau_k \subset \Theta} m(\tau_k)}{|\Theta| - 1} \\ &= \frac{1 - m(\tau_i)}{|\Theta| - 1}, \end{aligned} \tag{22}$$

where $|\Theta|$ is the cardinality of Θ.

Property 2. The DNBBA has the property of normalisation. The proof is as follows:

$$\begin{aligned} \sum_{\tau_i \subset \Theta} \bar{m}\ (\tau_i) &= \sum_{\tau_i \subset \Theta} \sum_{\tau_k \subset \Theta} m(\tau_k)\psi(\tau_i, \tau_k) \\ &= \sum_{\tau_k \subset \Theta} m(\tau_k) \left(\sum_{\tau_i \subset \Theta} \psi(\tau_i, \tau_k) \right), \end{aligned} \tag{23}$$

with

$$\sum_{\tau_i \subset \Theta} \psi(\tau_i, \tau_k) = 1. \tag{24}$$

Therefore,

$$\sum_{\tau_i \subset \Theta} \bar{m}\ (\tau_i) = \sum_{\tau_k \subset \Theta} m(\tau_k) \cdot 1 = \sum_{\tau_k \subset \Theta} m(\tau_k) = 1. \tag{25}$$

Theorem 2. Let $\bar{m}$ be a double negation of m. The process of the DNBBA is not involutionary when $|\Theta| > 2$, such that $\bar{\bar{m}}\ (\tau_i) \neq m(\tau_i)$. The proof is as follows:

$$\begin{aligned} \bar{\bar{m}}\ (\tau_i) &= \frac{1 - \bar{m}\ (\tau_i)}{|\Theta| - 1} \\ &= \frac{|\Theta| - 1 - (1 - m(\tau_i))}{(|\Theta| - 1)^2} \\ &= \frac{(|\Theta| - 2) + m(\tau_i)}{(|\Theta| - 1)^2}. \end{aligned} \tag{26}$$

When $|\Theta| > 2$, $\bar{\bar{m}}\ (\tau_i) \neq m(\tau_i)$ is clearly established.

Property 3. The DNBBA satisfies linear stability. When $m = \lambda m_1 + (1 - \lambda)m_2$ and $\sum_{\tau_k \subset \Theta} \psi(\tau_i, \tau_k) = 1$, $\bar{m} = \lambda\ \bar{m}_1 + (1 - \lambda)\ \bar{m}_2$. The proof is as follows:

$$\begin{aligned} \bar{m}\ (\tau_i) &= \sum_{\tau_k \subset \Theta} (\lambda m_1(\tau_k) + (1 - \lambda)m_2(\tau_k)) \cdot \psi(\tau_i, \tau_k) \\ &= \lambda \sum_{\tau_k \subset \Theta} m_1(\tau_k)\psi(\tau_i, \tau_k) \\ &+ (1 - \lambda) \sum_{\tau_k \subset \Theta} m_2(\tau_k)\psi(\tau_i, \tau_k) \\ &= \lambda\ \bar{m}_1\ (\tau_i) + (1 - \lambda)\ \bar{m}_2\ (\tau_i). \end{aligned} \tag{27}$$

Theorem 3. When $|\tau_i| = 1, \tau_i \cap \tau_k = \emptyset$. After the $(\upsilon + 1)^{th}$ negation, the negative iteration formula for m is as follows:

$$\bar{m}_{\upsilon+1} = \frac{1 - \bar{m}_{\upsilon}}{|\Theta| - 1}, \tag{28}$$

and $\bar{m}_{v+1}$ are subtracted from the value of the fixed point simultaneously

$$\begin{aligned}\bar{m}_{v+1} - \frac{1}{|\Theta|} &= \frac{1 - \bar{m}_v}{|\Theta| - 1} - \frac{1}{|\Theta|} \\ &= \frac{|\Theta| - |\Theta|\ \bar{m}_v - |\Theta| + 1}{|\Theta|(|\Theta| - 1)} \\ &= \frac{1 - |\Theta|\ \bar{m}_v}{|\Theta|(|\Theta| - 1)} \\ &= \frac{\bar{m}_v - \frac{1}{|\Theta|}}{1 - |\Theta|},\end{aligned} \tag{29}$$

where $\bar{m}_v - \frac{1}{|\Theta|}$ is the geometrical sequence denoted M_v. The common ratio is $\frac{1}{1-|\Theta|}$, and the first term is $M_1 = \bar{m}_1 - \frac{1}{|\Theta|}$. The $\bar{m}_v$ is as follows:

$$\begin{aligned}&\bar{m}_v - \frac{1}{|\Theta|} = (\bar{m}_1 - \frac{1}{|\Theta|})(\frac{1}{1 - |\Theta|})^{v-1} \\ &\Rightarrow \bar{m}_v = (\bar{m}_1 - \frac{1}{|\Theta|})(\frac{1}{1 - |\Theta|})^{v-1} + \frac{1}{|\Theta|}.\end{aligned} \tag{30}$$

Corollary 1. When $v \to \infty$, $\bar{m}_i$ becomes a uniform distribution with the following formula:

$$\lim_{v \to \infty} \bar{m}_v = \frac{1}{|\Theta|}. \tag{31}$$

Property 4. The value of $\bar{m}\ (\tau_i)$ has an upper bound. The proof is as follows:

$$\begin{aligned}\sum_{\tau_i \subset \Theta} \sum_{\tau_k \subset \Theta} m(\tau_k) \cdot \psi(\tau_i, \tau_k) = 1, \\ \bar{m}\ (\tau_i) \leq \sum_{\tau_i \subset \Theta} \sum_{\tau_k \subset \Theta} m(\tau_k) \cdot \psi(\tau_i, \tau_k) = 1.\end{aligned} \tag{32}$$

Property 5. Since $\psi(\tau_i, \tau_k)$ is asymmetric, $\bar{m}$ is biased toward the direction with the most assignments away from the original. When BBAs are reversed, the information center of gravity shifts to play the role of refutation, which is consistent with the counter-questioning in the DST.

Property 6. The DNBBA inherently tends to increase in entropy. $\psi(\cdot)$ can distribute $m(\tau_k)$ smoothly across multiple τ_i, which makes $\bar{m}$ more dispersed than m and leads to an increase in the entropy of $\bar{m}$. The proof is as follows:

$$\begin{aligned}H(\bar{m}) &= -\sum_i \bar{m}_i \log \bar{m}_i \\ &= -\sum_i \left(\sum_k m_k \cdot \psi_{ik} \right) \log \left(\sum_k m_k \cdot \psi_{ik} \right).\end{aligned} \tag{33}$$

According to Jensen's inequality,

$$\begin{aligned}f\left(\mathbb{E}[X]\right) \leq \mathbb{E}[f(X)], f \text{ is a convex function}, \\ f\left(\mathbb{E}[X]\right) \geq \mathbb{E}[f(X)], f \text{ is a concave function},\end{aligned} \tag{34}$$

and $H(\cdot)$ is a concave function. The formula is as follows:

$$-\log \left(\sum_k \psi_{ik} m_k \right) \geq \sum_k \frac{\psi_{ik} m_k}{\bar{m}_i} \left(-\log m_k \right). \tag{35}$$

$$
\begin{aligned}
-\sum_i \bar{m}_i \log \bar{m}_i &\geq \sum_i \sum_k \psi_{ik} m_k (-\log m_k) \\
&= \sum_k m_k (-\log m_k) \sum_i \psi_{ik} \\
&= \sum_k m_k (-\log m_k),
\end{aligned} \tag{36}
$$

$$
H(\bar{m}) \geq H(m), \tag{37}
$$

where $\bar{m}_i$ denotes $\bar{m}\ (\tau_i)$, $\bar{m}_k$ denotes $\bar{m}\ (\tau_k)$, and ψ_{ik} denotes $\psi(\tau_i, \tau_k)$.

Property 7. The DNBBA satisfies the principle of minimal self-consistency. When τ_i has all the beliefs, $m(\tau_i) = 1$, $\bar{m}\ (\tau_i) = \psi(\tau_i, \tau_i) = 0$, which indicates that the dissimilarity between $m(\tau_i)$ and $m(\tau_i)$ is 0.

Property 8. The DNBBA has boundary behavior. When $\tau_i = \tau_k$, $\psi(\tau_i, \tau_k) = 0$, $\tau_i \cap \tau_k = \emptyset$, $\bar{\psi}_{max}\ (\tau_i, \tau_k) = \alpha + \beta$, the representation of $\bar{m}\ (\tau_i)$ is given as follows:

$$
\begin{aligned}
\bar{m}\ (\tau_i) &= \sum_{\tau_k \subset \Theta} m(\tau_k) \cdot \psi(\tau_i, \tau_k) \\
&= \sum_{\tau_i \neq \tau_k} m(\tau_k) \psi(\tau_i, \tau_k).
\end{aligned} \tag{38}
$$

Property 9. The negation of BBA is sensitive to set differences, and even if the union of two sets is large, the negation of BBA will be small if they have many different elements.

Property 10. The negative value of the BBA for each proposition is independent of the order of the elements in that proposition.

Table 7: Image datasets.

Dataset	Training	Test	Class	Size	Dataset	Training	Test
CIFAR-10	50000	10000	10	32	LOL-v1	485	15
MNIST	60000	10000	10	28	LOL-v2-real	689	100
Fashion-MNIST	60000	10000	10	28	LOL-v2-syn	900	100

A.3 More Details of Experimental Settings

To verify the effectiveness of the proposed method, experiments were conducted on two different types of datasets. In Table 8, five classic structured datasets, including Iris Veenman & Reinders (2005), Heart Xu et al. (2016), Hepatitis Xu et al. (2013), Parkinson's Little (2007), and Australian Xiao et al. (2023), were selected. The sample sizes ranged from 150 to 690, and the number of categories ranged from 2 to 3, with feature dimensions ranging from 4 to 22. This allowed for the effective verification of the method's performance on structured data of different scales and complexities. In Table 7, on the one hand, three general image classification benchmark datasets, CIFAR-10 Ganjdanesh et al. (2024), MNIST Li et al. (2025), and Fashion-MNIST Yang et al. (2024), were used. Their training set sizes ranged from 50,000 to 60,000, and the test set was 10,000. These were used to evaluate the model's general image classification ability. On the other hand, three low-light image enhancement specialized datasets, LOL-v1 Cai et al. (2023), LOL-v2-real Yang et al. (2021), and LOL-v2-synFan et al. (2025b), were selected. Their training and test splits were 485:15, 689:100, and 900:100, respectively, to test the performance of the method in specific visual tasks. All the experiments were run on NVIDIA RTX 3090 GPUs.

A.4 Broader Impacts

We propose a dynamic negation of basic belief assignment (DNBBA) for measuring refutation strength. In addition, the properties of DNBBA are analysed. On this basis, a decision-making network based on DNBBA (DNBBA-DNet) is proposed for pattern classification and low-light image enhancement, and its effectiveness in classification and enhancement tasks is verified. In addition,

Table 8: Table datasets.

Dataset	Sample	Class	Feature
Iris	150	3	4
Heart	270	2	13
Hepatitis	155	2	19
Parkinson's	197	2	22
Australian	690	2	14

for the first time, we incorporate the idea of basic belief negation into low-light image enhancement and consider the decision-making problem from the perspective of negation. For the purposes of this paper, our proposed method has no negative impact.